Neural Dynamics on Complex Networks

Chengxi Zang, Fei Wang
Department of Healthcare Policy and Research
Weill Cornell Medicine
chz4001@med.cornell.edu, few2001@med.cornell.edu

Abstract

We introduce a deep learning model to learn continuous-time dynamics on complex networks and infer the semantic labels of nodes in the network at terminal time. We formulate the problem as an optimal control problem by minimizing a loss function consisting of a running loss of network dynamics, a terminal loss of nodes' labels, and a neural-differential-equation-system constraint. We solve the problem by a differential deep learning framework: as for the forward process of the system, rather than forwarding through a discrete number of hidden layers, we integrate the ordinary differential equation systems on graphs over continuous time; as for the backward learning process, we learn the optimal control parameters by back-propagation during solving initial value problem. We validate our model by learning complex dynamics on various real-world complex networks, and then apply our model to graph semi-supervised classification tasks. The promising experimental results demonstrate our model's capability of jointly capturing the structure, dynamics and semantics of complex systems.

1 Introduction

Real-world complex systems, such as brain [18], ecological systems [17], gene regulation [2], economic system [22] and human health [5] etc., are usually modeled as complex networks and their evolution are driven by some underlying nonlinear dynamics [33]. Revealing such complex network dynamics is crucial for understanding the complex systems in nature. Effective analytical tools developed for this goal can further help us predict and control these complex systems.

Although the theory of (nonlinear) dynamics has been widely studied in different fields including applied math [41, 9], statistical physics [28], engineering [40], ecology [17] and biology [5], these developed models are typically based on clear knowledge of the network evolution mechanism (which are thus usually referred as *mechanistic models*). Given the complexity of the real world, there is still a large amount of complex networks whose underlying dynamics are unknown yet (e.g., they can be too complex to be models by explicit mathematical functions). At the same time, massive data are usually generated during the evolution of these networks. Therefore, modern data-driven approaches are promising and highly demanding in modeling the unknown dynamics of complex networks. Two key components for developing a successful data-driven approach for modeling the dynamics of complex network are 1) the interaction structure of the nodes in the complex networks; and 2) the rules governing the dynamic change of the nodes' states in the complex networks.

In this paper we propose a novel "differential" deep learning based approach to learn the continuous-time dynamics on complex networks [33] and simultaneously infer the unknown semantic labels of nodes with high-dimensional features [49] at terminal time. We formulate the problem as an optimal control problem [15] by minimizing the running loss of network dynamics and terminal loss of semantic labels of nodes. The constraint of this optimization problem is in the form of a neural differential equation system which enables learning optimal control parameters in a data-driven manner. One unique design of our framework is that instead of forwarding the flow of information

Preprint. Under review.

as in conventional neural network learning process through a discrete number of layers [26], we integrate the neural dynamics on graphs over continuous-time and then learn the differential equation systems which model the continuous-time network dynamics. This is like a deep neural network with infinite number of layers [10]. Moreover, our approach also gives the meanings of physical time and continuous-time network dynamics to the depth and hidden outputs of neural network structure respectively. In addition, we further enhance our algorithm, called neural dynamics on complex networks (NDCN), by learning the dynamics in the embedding space of the high-dimensional node features.

We validate our approach by answering two general questions: 1) *Can we learn the continuous-time dynamics on complex networks*? 2) *Can we infer the semantic labels of nodes at terminal time stamp*? The experimental results show that our model accurately learns the real-world (linear/nonlinear) dynamics (e.g., heat diffusion in physical world, mutualistic interaction dynamics in ecology, and gene regulatory dynamics) on various complex networks. To the best of our knowledge, our learning framework for complex network dynamics is the first one of its kind. Furthermore, our model learns the semantic labels of nodes in various real-world network datasets in the setting of graph based semi-supervised classification [49, 24] with superior performances. Our codes and datasets are open-sourced at Appendix A.

2 The General framework

We first introduce a differential equation system which models the dynamics on complex networks:

$$\frac{dX(t)}{dt} = f\Big(X(t), G, W(t), t\Big), \tag{1}$$

where $X(t) \in \mathbb{R}^{n\times d}$ represents the state of a dynamic system consisting of n linked nodes at time $t \in [0, \infty)$, and each node is characterized by d dimensional features. $G = (\mathcal{V}, \mathcal{E})$ is the network structure capturing how the nodes are linked to each other. $W(t)$ is the parameters controlling how the system evolves over time. $X(0) = X_0$ is the initial states (node feature values) of this system at time $t = 0$. The function $f : \mathbb{R}^{n\times d} \to \mathbb{R}^{n\times d}$ is a function governing the dynamics of the system, which could be either linear or nonlinear. By convention, we denotes $\frac{dX(t)}{dt} = f(X(t), G, W(t), t)$ as $\dot{X} = f(X, G, W, t)$ for simplicity. In addition, nodes can have various semantic labels $Y(X, \Theta, t) \in \{0, 1\}^{n\times k}$ at time t, and Θ represents the parameters of this classification function. The problems we are trying to solve in this paper are:

- *How to learn the dynamics $\dot{X(t)}$ of complex networks from empirical data?*
- *How to learn the semantic labels of $Y(X(t))$ at time stamp $t = T$ for each node?*

In order to solve these problems, we first formulate them as an optimal control problem so that the goal becomes to obtain 1) the best control parameters $W(t)$ for differential equation system $\dot{X} = f(X, G, W, t)$ and 2) the best classification parameters Θ for semantic function $Y(X(t), \Theta)$ simultaneously by solving the following optimization problem:

$$\begin{aligned} &\underset{W(t),\Theta(T)}{\operatorname{argmin}}\ \mathcal{L} = \int_0^T \mathcal{R}\Big(X(t), G, W(t), t\Big)\, dt + \mathcal{S}\Big(Y(X(T), \Theta)\Big) \\ &\text{subject to } \frac{dX(t)}{dt} = f\Big(X(t), G, W(t), t\Big),\ X_0 \end{aligned} \tag{2}$$

where $\mathcal{R}(X(t), G, W(t), t) = \mathcal{R}(X_0 + \int_0^t f(X(\tau), G, W(\tau), \tau)\ d\tau)$ is the *running loss* of the dynamics on graph at time t, and $\mathcal{S}(Y(X(T), \Theta)) = \mathcal{S}(Y(X_0 + \int_0^T f(X(\tau), G, W(\tau), \tau)\ d\tau,\ \Theta))$ is the *terminal semantic loss* at time stamp T. By integrating $\dot{X} = f(X, G, W, t)$ over time t from initial state X_0 (a.k.a. solving the initial value problem [9] for this differential equation system), we can get the $X(t)$ for any arbitrary time stamp $t > 0$.

An equivalent formulation of Eq.(2) by explicitly solving the initial value problem of differential equation system is:

$$\begin{aligned} &\underset{W(t),\Theta(T)}{\operatorname{argmin}}\ \mathcal{L} = \int_0^T \mathcal{R}\Big(X(t), G, W(t), t\Big)\, dt + \mathcal{S}\Big(Y(X(T), \Theta)\Big) \\ &\text{subject to } X(t) = X(0) + \int_0^t f\Big(X(\tau), G, W(\tau), \tau\Big)\, d\tau \end{aligned} \tag{3}$$

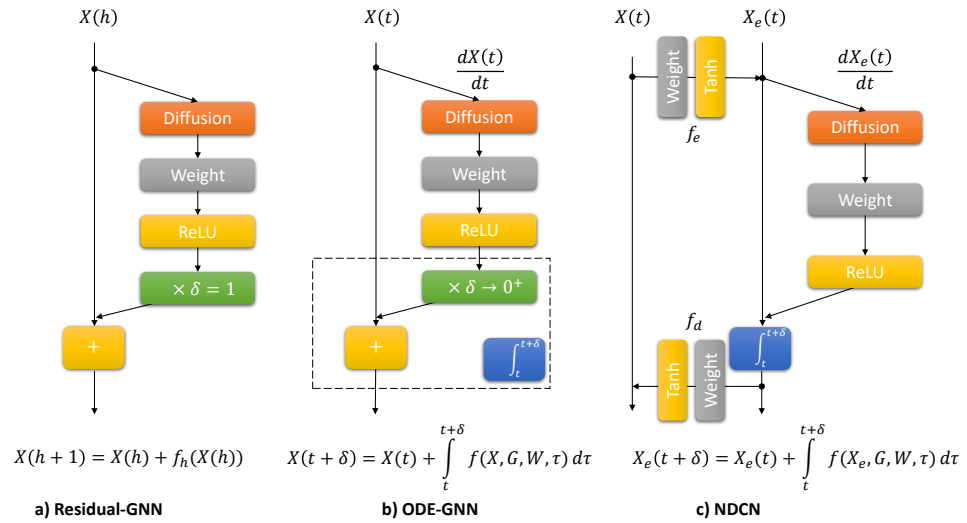

Figure 1: *Illustration of the modeling framework:* a) Residual Graph Neural Networks, b) ODE-GNN model and c) Our Neural Dynamics on Complex Network (NDCN) model. The h represents the discrete h^{th} layer and t represents continuous physical time.

Moreover, to further increase the expressability of the model, inspired by representation learning [7], embedding methods [11] and decoupling methods in differential equation theory, we can encode the network signal $X(t)$ from the original space to the transformed signal $X_e(t)$ in embedding space (usually with different number of dimensions), and learn the dynamics in such space. Then our model becomes:

$$\begin{aligned} \underset{W(t),\Theta(T)}{\text{argmin}} \quad & \mathcal{L} = \int_0^T \mathcal{R}\Big(X(t), G, W(t), t\Big)\, dt + \mathcal{S}\Big(Y(X(T), \Theta)\Big) \\ \text{subject to} \quad & X_e(t) = f_e\Big(X(t)\Big), \\ & X_e(t) = X_e(0) + \int_0^t f\Big(X_e(\tau), G, W(\tau), \tau\Big)\, d\tau, \\ & X(t) = f_d\Big(X_e(t)\Big) \end{aligned} \tag{4}$$

where first constraint encodes $X(t)$ into the embedded signal $X_e(t)$ through embedding function f_e. The second constraint is basically the initial value problem in the embedded space which governs the network dynamics. The third constraint decodes the embedded signal back to the original space with mapping function f_d.

We solve the initial value problem of integrating the differential equation systems numerically (e.g., by Dormand–Prince method DOPRI5 [12]) in the forward process, and backpropagate the gradients of the loss function w.r.t the control parameters over the numerical integration process backwards and solve the optimization problem by stochastic gradient descent methods (e.g., Adam [23]). We will show concrete examples of above framework by learning dynamics on complex networks, and learning the semantic labels of nodes' terminal states.

3 Learning dynamics on complex networks

In this section we are trying to answer the first question, *how to learn the (nonlinear) dynamics* $\dot{X(t)}$ *of complex networks from empirical data*. We will solve the problem (4) without emphasizing terminal loss $\mathcal{S}$ as no label information involved in this part. More concretely, without the loss of generality, we use ℓ_1-norm loss as the running loss $\mathcal{R}$, a fully connected neural network with a single hidden layer as the embedding function f_e, a graph neural network (GNN) structure [6] to model the instantaneous network dynamics in the embedding space, and a linear mapping function f_d. Thus,

our optimization problem becomes as follows and we illustrate the neural structures in the constraint as shown in Figure 1 :

$$\begin{aligned} \underset{W(t),b(t),W_e,b_e,W_d,b_d}{\operatorname{argmin}} \quad & \mathcal{L} = \int_0^T |X(t) - \hat{X(t)}| \, dt \\ \text{subject to} \quad & X_e(t) = \tanh\Big(X(t)W_e + b_e\Big)W(0) + b(0), \\ & X_e(t) = X_e(0) + \int_0^t \operatorname{ReLU}\Big(\Phi X_e(\tau)W(\tau) + b(\tau)\Big)\, d\tau, \\ & X(t) = X_e(t)W_d + b_d \end{aligned} \tag{5}$$

where $\hat{X(t)} \in \mathbb{R}^{n\times d}$ is the supervised dynamic information available at time stamp t (in the semi-supervised case the missing information can be padded by 0). The $|\cdot|$ denotes ℓ_1-norm loss (mean element-wise absolute value difference) between $X(t)$ and $\hat{X(t)}$ at time $t \in [0, T]$. $\Phi = D^{-\frac{1}{2}}(D - A)D^{-\frac{1}{2}} \in \mathbb{R}^{n\times n}$ is the diffusion operator in GNN, which is the normalized graph Laplacian constructed on the network. $A \in \mathbb{R}^{n\times n}$ is the adjacency matrix of the network and $D \in \mathbb{R}^{n\times n}$ is the corresponding node degree matrix. $W(t) \in \mathbb{R}^{d_e\times d_e}$ and $b(t) \in \mathbb{R}^{n\times d_e}$ are control parameters at time t (namely, the weights and bias of a linear connection layer at time t), $W_e \in \mathbb{R}^{d\times d_e}$ and $W_d \in \mathbb{R}^{d_e\times d}$ are the transformation matrices for encoding and decoding, and $b_d \in \mathbb{R}^{n\times d}$ is the bias at the decoding layer. For brevity, we call all the parameters $W(t), b(t), W_e, b_e, W_d, b_d$ as control parameters, or control, which need to be estimated from empirical data so that we can learn $\dot{X}$ in a data-driven manner. The neural differential equation system we used is $\dot{X(t)} = \operatorname{ReLU}(\Phi X(t)W(t) + b(t))$.

By applying the basic linear operator, which is the normalized graph Laplacian Φ, together with nonlinear activation function ReLU for differential equation systems in the embedding space, our model can capture various (linear or nonlinear) dynamics $\dot{X} = f(X, G, W, t)$ on different complex networks G accurately. Let $\overrightarrow{x_i(t)} \in \mathbb{R}^{d\times 1}$ be the d dimensional feature states of node i at time t and thus $X(t) = [\ldots, \overrightarrow{x_i(t)}, \ldots]^T$. We investigate following real-world network dynamics $\dot{X} = f(X, G, W, t)$:

- The heat diffusion dynamics governed by Newton's law of cooling [30], i.e.

$$\frac{d\overrightarrow{x_i(t)}}{dt} = -k_{i,j}\sum\nolimits_{j=1}^{n} A_{i,j}(\overrightarrow{x_i} - \overrightarrow{x_j}), \tag{6}$$

  which states that the rate of heat change of node i is proportional to the difference in the temperatures between i and its neighbors with heat capacity matrix A.
- The mutualistic interaction dynamics among species in ecology, governed by equation (For brevity, the operations between vectors are element-wise).

$$\frac{d\overrightarrow{x_i(t)}}{dt} = b_i + \overrightarrow{x_i}(1 - \frac{\overrightarrow{x_i}}{k_i})(\frac{\overrightarrow{x_i}}{c_i} - 1) + \sum_{j=1}^{n} A_{i,j}\frac{\overrightarrow{x_i}\overrightarrow{x_j}}{d_i + e_i\overrightarrow{x_i} + h_j\overrightarrow{x_j}}. \tag{7}$$

  The mutualistic differential equation systems [17] capture the abundance $\vec{x_i(t)}$ of species i, consisting of incoming migration term b_i, logistic growth with population capacity k_i [51] and Allee effect [1] with cold-start threshold c_i, and mutualistic interaction term with interaction network A.
- The gene regulatory dynamics governed by Michaelis-Menten equation [2]

$$\frac{d\overrightarrow{x_i(t)}}{dt} = -b_i\vec{x_i}^f + \sum\nolimits_{j=1}^{n} A_{i,j}\frac{\overrightarrow{x_j}^h}{\overrightarrow{x_j}^h + 1} \tag{8}$$

  where the first term models degradation when $f = 1$ or dimerization when $f = 2$, and the second term captures genetic activation tuned by the Hill coefficient h [17].

Please refer to Appendix B for the animations of these dynamics on various complex networks.

3.1 Experiments

We first investigate whether our NDCN model can correctly learn the above dynamics on following networks: (a) Grid network, where each node is connected with 8 neighbors (adjacency matrix shown

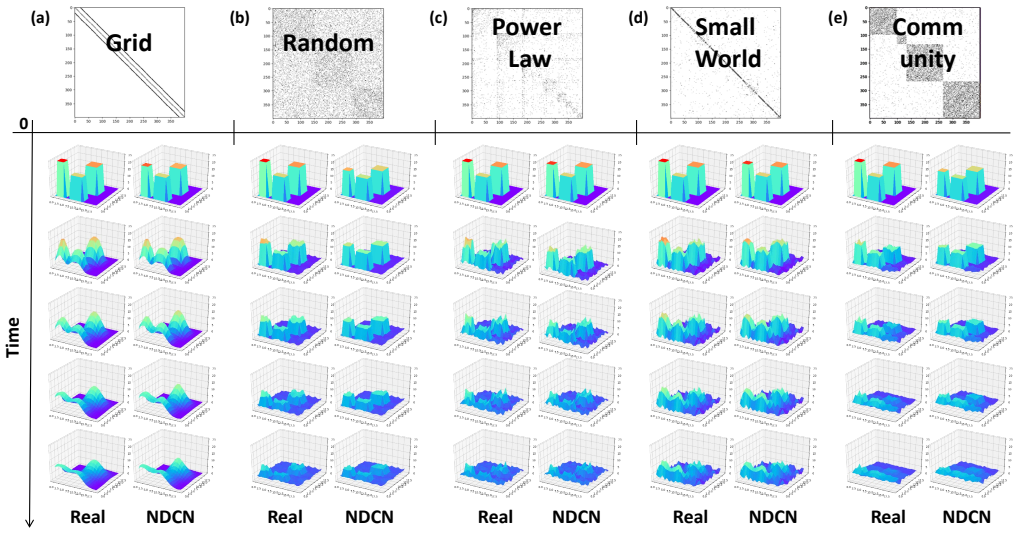

Figure 2: *Heat diffusion on different networks.* Each of the five vertical panel represents the dynamics on one network over physical time. For each network dynamics, we illustrate the sampled ground truth dynamics (left) and the dynamics generated by our NDCN (right) from top to down following the direction of time.

in Fig. 2(a)) [19]; (b) Random network, which is generated by Erdós and Rényi model [14] (adjacency matrix shown in Fig. 2(b)); (c) Power-law network, whigenerated by Albert-Barabási model [3] (adjacency matrix shown in Fig. 2(c)); (d) Small-world network, which is generated by Watts-Strogatz model [45] (adjacency matrix shown in Fig. 2(d)); and (e) Community network, generated by random partition model [16] (adjacency matrix shown in Fig. 2(e)).

Baselines. We compare our NDCN by investigating whether the embedding, graph operator, control parameters are indispensable, i.e. can our model still work well without any of these components. We keep the loss function the same and construct the following baselines:

- No-embedding model $X(t) = X(0) + \int_0^t \mathrm{ReLU}(\Phi X(\tau)W(\tau) + b(\tau))\, d\tau$, namely ODE-GNN, which learns the dynamics in the original state space $X(t)$;
- No-graph-operator model $X_e(t) = X_e(0) + \int_0^t \mathrm{ReLU}(X_e(\tau)W(\tau) + b(\tau))\, d\tau$, $X_e(t) = \tanh(X(t)W_e + b_e)W(0) + b(0)$, $X(t) = X_e(t)W_d + b_d$, namely ODE-NN, which can be thought as a continuous-time residual (differential) neural network without considering the network structure;
- No-control-parameter model $X_e(t) = X_e(0) + \int_0^t \mathrm{ReLU}\left(\Phi X_e(\tau)\right)\, d\tau$, $X_e(t) = \tanh(X(t)W_e + b_e)W(0) + b(0)$, $X(t) = X_e(t)W_d + b_d$, which has no linear connection layer between t and $t + dt$ (where $dt \to 0$) in the running dynamics and only keeps the parameters in the embedding layers.

Experimental setup. We first generate networks by aforementioned network models with 400 nodes. The nodes are re-ordered according to community detection method by Newman [32]. We visualize their adjacency matrices in Fig. 2,3 and 4. We layout these networks in a grid and thus nodes' states $X(t)$ are visualized as functions on the grid. We set the initial value $X(0)$ the same for all the experimental settings and thus different dynamics are only due to their different dynamic rules and underlying networks modelled by $\dot{X} = f(X, G, W, t)$ as shown in Fig. 2,3 and 4. The supervised information $\hat{X(t)}$ are 20 evenly-spaced-sampled dynamics during $[0, T]$. Please kindly refer to Appendix B for the animations of all the network dynamics and their detailed configurations. We choose 20 as the embedding dimensionality. We solve the initial value problem of integrating the differential equation systems numerically by Dormand–Prince method DOPRI5 [12] in the forward process. We train our model for a maximum of 2000 epochs using Adam [23] with learning rate 0.01 and ℓ_2 regularization parameter set to 0.001. We evaluate the results by standard ℓ_1 loss, namely

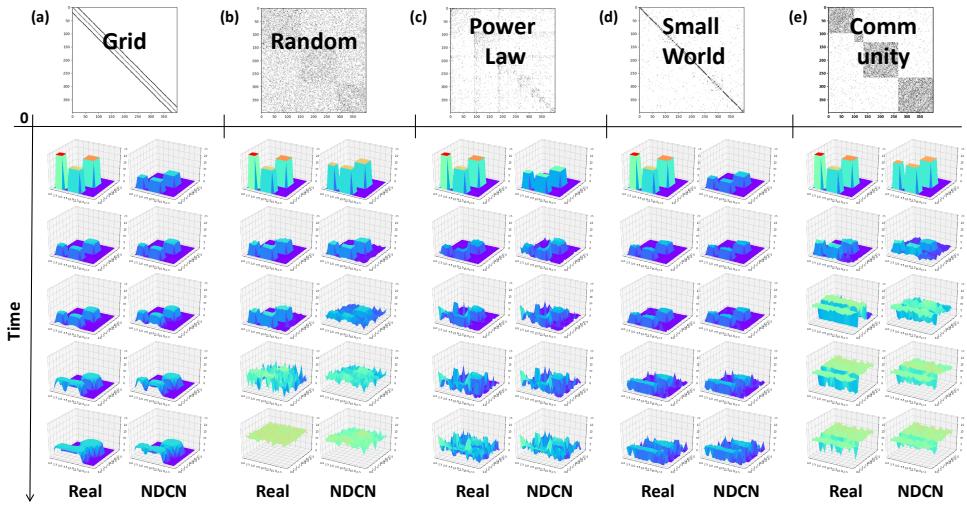

Figure 3: *Biological mutualistic interaction on different networks.*

mean element-wise absolute value difference between $X(t)$ and $\hat{X}(t)$ over $t \in [0, T]$ and normalized ℓ_1 loss normalized by the mean element-wise value of $\hat{X}(t)$, and they lead to the same conclusion. For the ease of comparison, we report normalized ℓ_1 loss in Table 1 (See Appendix C.1 for the absolute error). Results are mean and standard deviation of the loss over 20 independent runs.

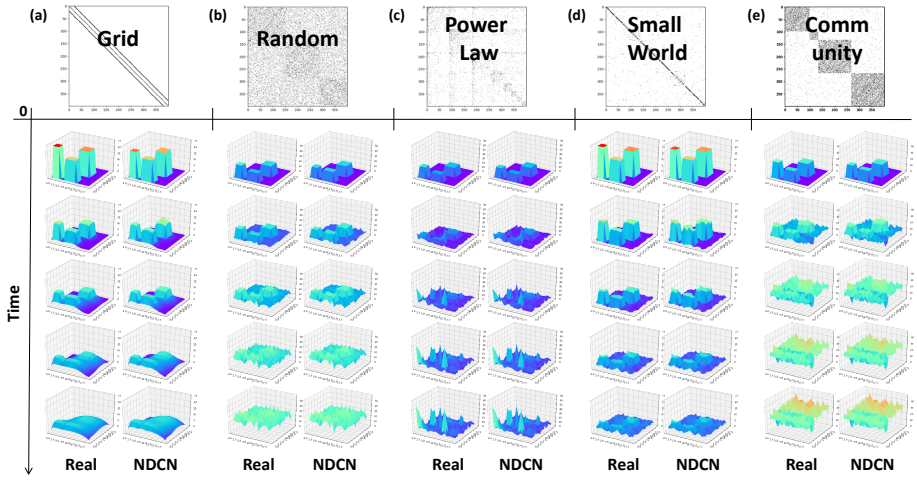

Figure 4: *Gene regulation dynamics on different networks.*

3.2 Results

The numerical results are summarized in Table 1 and the visualization of the learned dynamics are shown in Fig. 2,3 and 4 (See the animations of these network dynamics in Appendix B). We can observe that our NDCN captures different dynamics on various complex networks accurately and outperforms all baselines, namely the models without embedding, control parameters or graph operator, by a large margin, indicating that our NDCN potentially serves as a minimal model in learning dynamics on complex networks.

We also examine other experimental settings in $\dot{X} = f(X, G, W, t)$: (a) other activation functions like hyperbolic tangent function $\tanh$; (b) graph operator including Laplacian without being normalized, convolution operator adopted in graph convolution neural network [24], etc.; (c) different numerical integration method for initial value problem like Euler's method [9], etc.; they all get worse results than our model and we do not report them here for brevity (Appendix C).

Table 1: Our NDCN captures different network dynamics accurately. The mean fitting errors with standard deviation (in percentage $\%$) in 20 runs measured by normalized ℓ_1 loss.

		Grid	Random	Power Law	Small World	Community
Heat Diffusion	No-Embedding	28.7 ± 9.2	29.1 ± 0.5	28.4 ± 2.3	27.5 ± 5.1	32.9 ± 2.7
	No-Graph	39.5 ± 1.8	10.5 ± 1.4	15.8 ± 0.6	22.3 ± 0.5	27.1 ± 1.9
	No-Control	60.7 ± 0.9	34.8 ± 0.0	34.5 ± 0.5	39.9 ± 0.2	41.3 ± 0.4
	NDCN	$\mathbf{3.9 \pm 0.7}$	$\mathbf{7.2 \pm 0.2}$	$\mathbf{5.4 \pm 0.7}$	$\mathbf{3.4 \pm 0.6}$	$\mathbf{9.4 \pm 0.7}$
Mutualistic Interaction	No-Embedding	37.3 ± 4.5	19.5 ± 1.8	35.6 ± 12.6	35.9 ± 3.1	22.7 ± 4.1
	No-Graph	39.6 ± 7.3	8.9 ± 3.0	23.4 ± 3.3	35.8 ± 3.0	14.0 ± 1.0
	No-Control	81.2 ± 0.8	21.6 ± 0.3	57.5 ± 0.1	75.5 ± 0.7	30.9 ± 0.1
	NDCN	$\mathbf{11.3 \pm 1.8}$	$\mathbf{5.8 \pm 0.6}$	$\mathbf{9.2 \pm 0.7}$	$\mathbf{12.0 \pm 1.4}$	$\mathbf{6.8 \pm 0.4}$
Gene Regulation	No-Embedding	34.9 ± 10.8	12.0 ± 7.8	33.4 ± 9.1	28.0 ± 9.6	20.7 ± 7.8
	No-Graph	29.4 ± 33.8	12.3 ± 0.9	39.9 ± 1.0	15.8 ± 0.5	19.4 ± 0.2
	No-Control	61.9 ± 0.2	35.7 ± 0.4	45.0 ± 0.1	48.2 ± 0.1	39.6 ± 0.5
	NDCN	$\mathbf{6.3 \pm 0.6}$	$\mathbf{1.3 \pm 0.3}$	$\mathbf{2.8 \pm 0.2}$	$\mathbf{4.9 \pm 0.4}$	$\mathbf{2.1 \pm 0.3}$

4 Learning terminal semantic labels

In this section we investigate the second question, i.e., *how to learn the semantic labels of each node at terminal time?* Here we consider the problem of semi-supervised classification on graphs [49, 24]. By leveraging both the network structure and the semantic features of linked nodes, various graph neural network (GNN) [6] approaches can achieve the state-of-the-art performance in inferring the unknown labels of nodes. However, existing GNNs usually adopt 1 or 2 hidden layers [24, 44] and cannot go deep [27]. Our framework go beyond an integer number L of hidden layers in GNNs to a real continuous depth t of hidden layers, implying continuous-time dynamics on graphs. We also observe that by integrating continuous-time dynamics over graph, we get more fine-grained forward process and thus our NDCN model shows very competitive even better results compared with state-of-the-art GNN models which may have sophisticated parameters (e.g. attention).

Following the same framework as in Section 3, we propose a specific model to achieve this goal by solving the following optimization problem, where the terminal semantic loss $\mathcal{S}(Y(T))$ is modeled by the standard cross-entropy loss for classification task:

$$\begin{aligned} \underset{W_e, b_e, W_d, b_d}{\operatorname{argmin}} \quad & \mathcal{L} = \int_0^T \mathcal{R}(t)\, dt - \sum_{i=1}^{n} \sum_{k=1}^{c} \hat{Y}_{i,k}(T) \log Y_{i,k}(T) \\ \text{subject to} \quad & X_e(t) = \tanh\Big(X(t) W_e + b_e\Big), \\ & X_e(t) = X_e(0) + \int_0^t \operatorname{ReLU}\Big(\Phi X_e(\tau)\Big)\, d\tau, \\ & Y(t) = \operatorname{softmax}(X_e(t) W_d + b_d) \end{aligned} \tag{9}$$

where $Y(t) \in \mathbb{R}^{n \times c}$ is the label distributions of nodes at time T whose element $Y_{i,k}(t)$ denotes the probability of the node $i = 1, \ldots, n$ with label $k = 1, \ldots, c$ at time t. The $\hat{Y} \in \mathbb{R}^{n \times c}$ is the supervised information (again missing information can be padded by 0) observed at time T. We use differential equation system $\dot{X}(t) = \operatorname{ReLU}(\Phi X(t))$.

Faced with limited semi-supervised data at a single snapshot, in order to learn a model with better generalization performance and avoid over-fitting, we: a) model the running loss $\int_0^T \mathcal{R}(t)\, dt$ as the ℓ_2-norm regularizer of the control parameters, and b) make more realistic assumptions of the unknown network dynamics to eliminate the overdose of the control parameters. Here, we only keep the control parameters in the embedding layers and thus $\int_0^T \mathcal{R}(t)\, dt = \lambda(|W_e|_2^2 + |b_e|_2^2 + |W_d|_2^2 + |b_d|_2^2)$. We adopt the diffusion operator $\Phi = \tilde{D}^{-\frac{1}{2}}(\alpha I + (1-\alpha)A)\tilde{D}^{-\frac{1}{2}}$ where A is the adjacency matrix, D is the degree matrix and $\tilde{D} = \alpha I + (1-\alpha)D$ keeps Φ normalized. The parameter $\alpha \in [0, 1]$ tunes nodes' adherence to their previous information or their neighbors' collective opinion. The differential equation system $\dot{X} = \Phi X$ follows the dynamics of averaging the neighborhood opinion as $\frac{d\overrightarrow{x_i(t)}}{dt} = \frac{\alpha}{(1-\alpha)d_i + \alpha}\overrightarrow{x_i(t)} + \sum_j^n A_{i,j} \frac{1-\alpha}{\sqrt{(1-\alpha)d_i+\alpha}\sqrt{(1-\alpha)d_j+\alpha}}\overrightarrow{x_j(t)}$ for node i. When $\alpha = 0$, Φ averages the neighbors as normalized random walk, when $\alpha = 1$, Φ captures exponential dynamics without network effects, and when $\alpha = 0.5$, Φ averages both neighbors and itself as in [24].

4.1 Experiments

Table 2: Statistics for three real-world citation network datasets. N, E, D, C represent number of nodes, edges, features, classes respectively.

Dataset	N	E	D	C	Train/Valid/Test
Cora	$2,708$	$5,429$	$1,433$	7	$140/500/1,000$
Citeseer	$3,327$	$4,732$	$3,703$	6	$120/500/1,000$
Pubmed	$19,717$	$44,338$	500	3	$60/500/1,000$

We validate our model in graph semi-supervised classification setting, which infers the node semantic labels given the underlying graph, nodes' features and few supervised labels of nodes. We find by capturing the continuous-time dynamics, our NDCN model shows very competitive even better results compared with state-of-the-art GNNs with sophisticated parameters. Besides, we DO NOT use common deep learning techniques adopted in previous GNN models, including dropout, connections between layers, and the concept of layer depth. Our model is all about continuous-time Neural Dynamics on Complex Networks/graphs (NDCN).

Datasets. Three standard benchmark datasets, namely citation network Cora, Citeseer and Pubmed [49] are used. We follow the same fixed split scheme for train, validation and test datasets for comparison as in [49, 24, 43]. We summarize the datasets in Table 2.

Baselines. We compare our NDCN model with graph embedding method DeepWalk [34] and the state-of-the-art GNN models, including graph convolution network (GCN) [24], attention-based graph neural network (AGNN) [43], and graph attention networks (GAT) [44] with sophisticated attention parameters.

Experimental setup. For the consistency of comparison with prior work, we follow the same experimental setup as [24, 44, 43]. We train our model based on the training datasets and get the accuracy of classification results from the test datasets with $1,000$ labels as summarized in Table 2. Following hyperparameter settings apply to all the datasets. We set 16 evenly spaced time ticks in $[0, T]$ and solve the initial value problem of integrating the differential equation systems numerically by DOPRI5 [12]. We train our model for a maximum of 100 epochs using Adam [23] with learning rate 0.01 and ℓ_2-norm regularization 0.024. We grid search the best terminal time $T \in [0.5, 1.5]$ and the $\alpha \in [0, 1]$. We use 256 hidden dimension. We report the mean and standard deviation of results for 100 runs in Table 3. It's worthwhile to emphasize that in our model there is no running control parameters (i.e. linear connection layers in GNNs), no dropout (e.g., dropout rate 0.5 in GCN and 0.6 in GAT), no early stop, and no concept of layer/network depth (e.g., 2 layers in GCN and GAT).

4.2 Results

We summarize the results in Table 3. We find our NDCN outperforms many state-of-the-art GNN models. Results for the baselines are taken from [24, 44, 43, 47]. We report the mean and standard deviation of our results for 100 runs. We get our reported results in Table 3 when terminal time $T = 1.2$, $\alpha = 0$ for the Cora dataset, $T = 1.0$, $\alpha = 0.8$ for the Citeseer dataset, and $T = 1.1$, $\alpha = 0.4$ for the Pubmed dataset.

Table 3: Test mean accuracy with standard deviation in percentage (%) over 100 runs. Our model gives competitive even better results compared with many state-of-the-art Graph Neural Network (GNN) models.

Model	Cora	Citeseer	Pubmed
DeepWalk	70.7 ± 0.6	51.4 ± 0.5	76.8 ± 0.6
GCN	81.5	70.3	79.0
AGNN	83.1 ± 0.1	71.7 ± 0.1	$\mathbf{79.9 \pm 0.1}$
GAT	83.0 ± 0.7	72.5 ± 0.7	79.0 ± 0.3
NDCN	$\mathbf{83.3 \pm 0.6}$	$\mathbf{73.1 \pm 0.6}$	$\mathbf{79.8 \pm 0.4}$

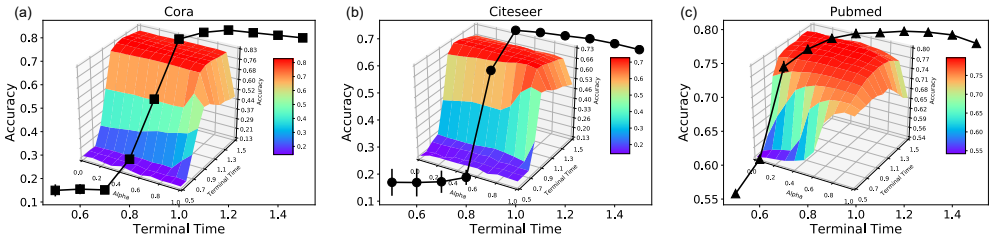

Figure 5: *Our NDCN model captures continuous-time dynamics.* Mean classification accuracy of 100 runs over terminal time when given a specific α. Insets are the accuracy over the two-dimensional space of terminal time and α

By capturing the continuous-time network dynamics, our NDCN gives better classification accuracy at terminal time $T \in \mathbb{R}^+$. Indeed, when the terminal time is too small or too large, the accuracy degenerates due to the fact that the features of nodes are in under-diffusion, or over-diffusion states. Figure 5 plots the mean accuracy (100 runs) with error bars over terminal time T in the abovementioned α settings (we further plot the accuracy over terminal time T and α in the insets

and Appendix D), we find for all the three datasets their accuracy curves follow rise and fall pattern around the best terminal time. In contrast, previous GNNs can only have integer number of layers which can not capture the continuous-time network dynamics accurately.

5 Related work

Dynamics of complex systems. Real-world complex systems are modeled by complex networks and driven by nonlinear dynamics [33]. The dynamics of brain and human microbial are examined in [18] and [5] respectively. [17] and [28] investigated the resilience patterns and controllability of complex systems respectively. [4] gave a pipeline to construct network dynamics. To the best of our knowledge, our NDCN model is the first neural network approach which learns the dynamics of complex networks in a data-driven manner.

Data-driven dynamics. Recently, some data-driven approaches are proposed to learn ODEs or PDEs, including sparse regression [25], residual network [35], feedforward neural network [37], coupled neural networks [36] and so on. [31] tries to learn biological networks dynamics by sparse regression over a large library, which is not scalable to systems with more than 10 nodes. In all, none of them can learn the dynamics of complex systems with more than hundreds of nodes.

Neural ODEs. Inspired by residual network [21] and ordinary differential equation (ODE) theory [29, 39], seminal work neural ODE model [10] was proposed to re-write residual networks, normalizing flows, and recurrent neural network decoders by integrating the differential equations over time in the forward process of deep learning framework. See improved Neural ODEs in [13]. However, our NDCN model deals with complex differential equations systems. Besides, our model solves different problems, namely learning the dynamics of complex systems and semantic labels of their nodes at terminal time.

Optimal control. Relationships between back-propagation in deep learning [38] and optimal control theory [15] are investigated in [46, 20, 8]. We formulate our loss function by leveraging the concept of running loss and terminal loss in optimal control. We give a novel constraint in optimal control which is modeled by neural differential equations systems on graphs. Novel tasks learning the running dynamics on complex networks and inferring the terminal labels are done by our NDCN in a data-driven manner.

Graph neural networks. Graph neural networks (GNN) [48] aim at applying deep learning techniques to graph data consisting of linked objects. Graph convolution network (GCN) [24], attention-based graph neural network (AGNN) [43], graph attention networks (GAT) [44] etc. achieved state-of-the-art performance on semi-supervised classification task on graphs. However, GNNs have usually 1 or 2 layers and can not go deep[27, 48]. Our NDCN gives a novel perspective on GNNs: we give the meanings of physical time and the continuous-time network dynamics to the layers and the hidden outputs respectively. By capturing continuous-time dynamics, we outperform above state-of-the-art GNNs in our second task. By combining RNN and GNN, [50] tries to predict the spatial-temporal data. The RNN leans discrete sequential samples by iterative mapping and our ODE method learns the continuous-time dynamics by integrating over physical time for physical processes in the real world [42].

6 Conclusion

We propose a novel neural network model to learn continuous-time dynamics on complex networks and infer the semantic labels of nodes at terminal time. We formulate the problem as an optimal control problem and propose a neural differential equations systems structure as the constraints of the optimization problem. By capturing the continuous-time network dynamics, our NDCN gives the meanings of physical time and the continuous-time network dynamics to the neural network framework, learns real-world complex network dynamics accurately, and outperforms many state-of-the-art GNN models in the graph semi-supervised classification task. Codes and datasets are open-sourced at Appendix A.

References

[1] Warder Clyde Allee, Orlando Park, Alfred Edwards Emerson, Thomas Park, Karl Patterson Schmidt, et al. Principles of animal ecology. Technical report, Saunders Company Philadelphia, Pennsylvania, USA, 1949.

[2] Uri Alon. *An introduction to systems biology: design principles of biological circuits*. Chapman and Hall/CRC, 2006.

[3] Albert-László Barabási and Réka Albert. Emergence of scaling in random networks. *science*, 286(5439):509–512, 1999.

[4] Baruch Barzel, Yang-Yu Liu, and Albert-László Barabási. Constructing minimal models for complex system dynamics. *Nature communications*, 6:7186, 2015.

[5] Amir Bashan, Travis E Gibson, Jonathan Friedman, Vincent J Carey, Scott T Weiss, Elizabeth L Hohmann, and Yang-Yu Liu. Universality of human microbial dynamics. *Nature*, 534(7606):259, 2016.

[6] Peter W Battaglia, Jessica B Hamrick, Victor Bapst, Alvaro Sanchez-Gonzalez, Vinicius Zambaldi, Mateusz Malinowski, Andrea Tacchetti, David Raposo, Adam Santoro, Ryan Faulkner, et al. Relational inductive biases, deep learning, and graph networks. *arXiv preprint arXiv:1806.01261*, 2018.

[7] Yoshua Bengio, Aaron Courville, and Pascal Vincent. Representation learning: A review and new perspectives. *IEEE transactions on pattern analysis and machine intelligence*, 35(8):1798–1828, 2013.

[8] Martin Benning, Elena Celledoni, Matthias J Ehrhardt, Brynjulf Owren, and Carola-Bibiane Schönlieb. Deep learning as optimal control problems: models and numerical methods. *arXiv preprint arXiv:1904.05657*, 2019.

[9] William E Boyce, Richard C DiPrima, and Douglas B Meade. *Elementary differential equations and boundary value problems*, volume 9. Wiley New York, 1992.

[10] Tian Qi Chen, Yulia Rubanova, Jesse Bettencourt, and David K Duvenaud. Neural ordinary differential equations. In *Advances in Neural Information Processing Systems*, pages 6571–6583, 2018.

[11] Peng Cui, Xiao Wang, Jian Pei, and Wenwu Zhu. A survey on network embedding. *IEEE Transactions on Knowledge and Data Engineering*, 2018.

[12] John R Dormand. *Numerical methods for differential equations: a computational approach*, volume 3. CRC Press, 1996.

[13] Emilien Dupont, Arnaud Doucet, and Yee Whye Teh. Augmented neural odes. *arXiv preprint arXiv:1904.01681*, 2019.

[14] P ERDdS and A R&wi. On random graphs i. *Publ. Math. Debrecen*, 6:290–297, 1959.

[15] Lawrence C Evans. An introduction to mathematical optimal control theory version 0.2. *Lecture notes available at http://math. berkeley. edu/˜ evans/control. course. pdf*, 1983.

[16] Santo Fortunato. Community detection in graphs. *Physics reports*, 486(3-5):75–174, 2010.

[17] Jianxi Gao, Baruch Barzel, and Albert-László Barabási. Universal resilience patterns in complex networks. *Nature*, 530(7590):307, 2016.

[18] Wulfram Gerstner, Werner M Kistler, Richard Naud, and Liam Paninski. *Neuronal dynamics: From single neurons to networks and models of cognition*. Cambridge University Press, 2014.

[19] Robert M Gray et al. Toeplitz and circulant matrices: A review. *Foundations and Trends® in Communications and Information Theory*, 2(3):155–239, 2006.

[20] Jiequn Han, Qianxiao Li, et al. A mean-field optimal control formulation of deep learning. *arXiv preprint arXiv:1807.01083*, 2018.

[21] Kaiming He, Xiangyu Zhang, Shaoqing Ren, and Jian Sun. Deep residual learning for image recognition. In *Proceedings of the IEEE conference on computer vision and pattern recognition*, pages 770–778, 2016.

[22] Michał Kalecki. *Theory of economic dynamics*. Routledge, 2013.

[23] Diederik P. Kingma and Jimmy Ba. Adam: A method for stochastic optimization. In *3rd International Conference on Learning Representations, ICLR 2015, San Diego, CA, USA, May 7-9, 2015, Conference Track Proceedings*, 2015.

[24] Thomas N. Kipf and Max Welling. Semi-supervised classification with graph convolutional networks. In *5th International Conference on Learning Representations, ICLR 2017, Toulon, France, April 24-26, 2017, Conference Track Proceedings*, 2017.

[25] J Nathan Kutz, Samuel H Rudy, Alessandro Alla, and Steven L Brunton. Data-driven discovery of governing physical laws and their parametric dependencies in engineering, physics and biology. In *2017 IEEE 7th International Workshop on Computational Advances in Multi-Sensor Adaptive Processing (CAMSAP)*, pages 1–5. IEEE, 2017.

[26] Yann LeCun, Yoshua Bengio, and Geoffrey Hinton. Deep learning. *nature*, 521(7553):436, 2015.

[27] Qimai Li, Zhichao Han, and Xiao-Ming Wu. Deeper insights into graph convolutional networks for semi-supervised learning. In *Thirty-Second AAAI Conference on Artificial Intelligence*, 2018.

[28] Yang-Yu Liu, Jean-Jacques Slotine, and Albert-László Barabási. Controllability of complex networks. *nature*, 473(7346):167, 2011.

[29] Yiping Lu, Aoxiao Zhong, Quanzheng Li, and Bin Dong. Beyond finite layer neural networks: Bridging deep architectures and numerical differential equations. *arXiv preprint arXiv:1710.10121*, 2017.

[30] A v Luikov. *Analytical heat diffusion theory*. Elsevier, 2012.

[31] Niall M Mangan, Steven L Brunton, Joshua L Proctor, and J Nathan Kutz. Inferring biological networks by sparse identification of nonlinear dynamics. *IEEE Transactions on Molecular, Biological and Multi-Scale Communications*, 2(1):52–63, 2016.

[32] Mark Newman. *Networks: an introduction*. Oxford university press, 2010.

[33] Mark Newman, Albert-Laszlo Barabasi, and Duncan J Watts. *The structure and dynamics of networks*, volume 12. Princeton University Press, 2011.

[34] Bryan Perozzi, Rami Al-Rfou, and Steven Skiena. Deepwalk: Online learning of social representations. In *Proceedings of the 20th ACM SIGKDD international conference on Knowledge discovery and data mining*, pages 701–710. ACM, 2014.

[35] Tong Qin, Kailiang Wu, and Dongbin Xiu. Data driven governing equations approximation using deep neural networks. *arXiv preprint arXiv:1811.05537*, 2018.

[36] Maziar Raissi. Deep hidden physics models: Deep learning of nonlinear partial differential equations. *The Journal of Machine Learning Research*, 19(1):932–955, 2018.

[37] Maziar Raissi, Paris Perdikaris, and George Em Karniadakis. Multistep neural networks for data-driven discovery of nonlinear dynamical systems. *arXiv preprint arXiv:1801.01236*, 2018.

[38] David E Rumelhart, Geoffrey E Hinton, Ronald J Williams, et al. Learning representations by back-propagating errors. *Cognitive modeling*, 5(3):1, 1988.

[39] Lars Ruthotto and Eldad Haber. Deep neural networks motivated by partial differential equations. *arXiv preprint arXiv:1804.04272*, 2018.

[40] Jean-Jacques E Slotine, Weiping Li, et al. *Applied nonlinear control*, volume 199. Prentice hall Englewood Cliffs, NJ, 1991.

[41] Steven H Strogatz. *Nonlinear Dynamics and Chaos with Student Solutions Manual: With Applications to Physics, Biology, Chemistry, and Engineering*. CRC Press, 2018.

[42] Corentin Tallec and Yann Ollivier. Can recurrent neural networks warp time? *arXiv preprint arXiv:1804.11188*, 2018.

[43] Kiran K Thekumparampil, Chong Wang, Sewoong Oh, and Li-Jia Li. Attention-based graph neural network for semi-supervised learning. *arXiv preprint arXiv:1803.03735*, 2018.

[44] Petar Veličković, Guillem Cucurull, Arantxa Casanova, Adriana Romero, Pietro Lio, and Yoshua Bengio. Graph attention networks. *arXiv preprint arXiv:1710.10903*, 2017.

[45] Duncan J Watts and Steven H Strogatz. Collective dynamics of 'small-world'networks. *nature*, 393(6684):440, 1998.

[46] E Weinan. A proposal on machine learning via dynamical systems. *Communications in Mathematics and Statistics*, 5(1):1–11, 2017.

[47] Felix Wu, Tianyi Zhang, Amauri H. Souza Jr., Christopher Fifty, Tao Yu, and Kilian Q. Weinberger. Simplifying graph convolutional networks. *CoRR*, 2019.

[48] Zonghan Wu, Shirui Pan, Fengwen Chen, Guodong Long, Chengqi Zhang, and Philip S Yu. A comprehensive survey on graph neural networks. *arXiv preprint arXiv:1901.00596*, 2019.

[49] Zhilin Yang, William W. Cohen, and Ruslan Salakhutdinov. Revisiting semi-supervised learning with graph embeddings. In *Proceedings of the 33nd International Conference on Machine Learning, ICML 2016, New York City, NY, USA, June 19-24, 2016*, pages 40–48, 2016.

[50] Bing Yu, Haoteng Yin, and Zhanxing Zhu. Spatio-temporal graph convolutional networks: A deep learning framework for traffic forecasting. *arXiv preprint arXiv:1709.04875*, 2017.

[51] Chengxi Zang, Peng Cui, Christos Faloutsos, and Wenwu Zhu. On power law growth of social networks. *IEEE Transactions on Knowledge and Data Engineering*, 30(9):1727–1740, 2018.

A Reproducibility

To ensure the reproducibility, we open-sourced our datasets and Pytorch implementation empowered by GPU and sparse matrix at:

B Animations of the real-world dynamics on different networks

Please view the animations of the three real-world dynamics on five different networks learned by different models at:

`https://drive.google.com/open?id=1KBl-6Oh7BRxcQNQrPeHuKPPI6lndDa5Y`

We will find our NDCN captures the real-world dynamics on different networks very accurately while the baselines can not. The detailed experimental configurations are shown as follows:

Underlying Networks: We generate various networks by as follows, and we visualize their adjacency matrix after re-ordering their nodes by the community detection method by Newman [32].

- Grid network:

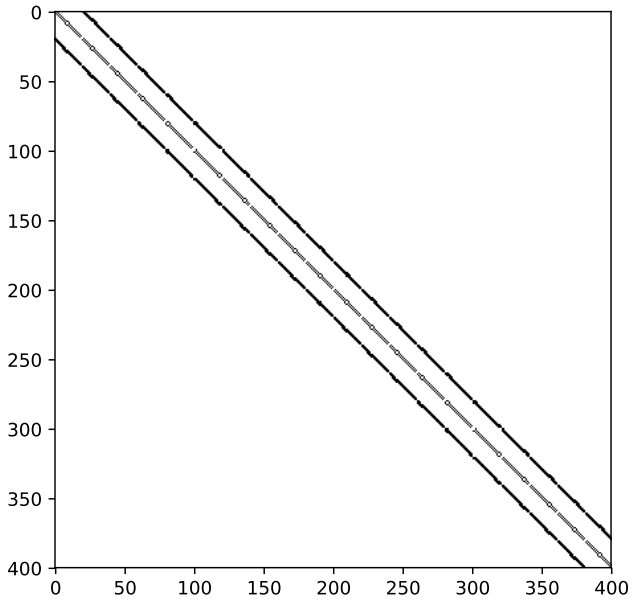

Figure 6: Adjacency matrix of grid network taking on a circulant matrix [19].

```
def grid_8_neighbor_graph(N):
    """
    Build discrete grid graph, each node has 8 neighbors
    :param n:  sqrt of the number of nodes
    :return:  A, the adjacency matrix
    """
    N = int(N)
    n = int(N ** 2)
    dx = [-1, 0, 1, -1, 1, -1, 0, 1]
    dy = [-1, -1, -1, 0, 0, 1, 1, 1]
    A = torch.zeros(n, n)
    for x in range(N):
        for y in range(N):
            index = x * N + y
            for i in range(len(dx)):
```

```
                newx = x + dx[i]
                newy = y + dy[i]
                if N > newx >= 0 and N > newy >= 0:
                    index2 = newx * N + newy
                    A[index, index2] = 1
    return A.float()
n = 400
N = int(np.ceil(np.sqrt(n)))
A = grid_8_neighbor_graph(N)
```

- Random network:

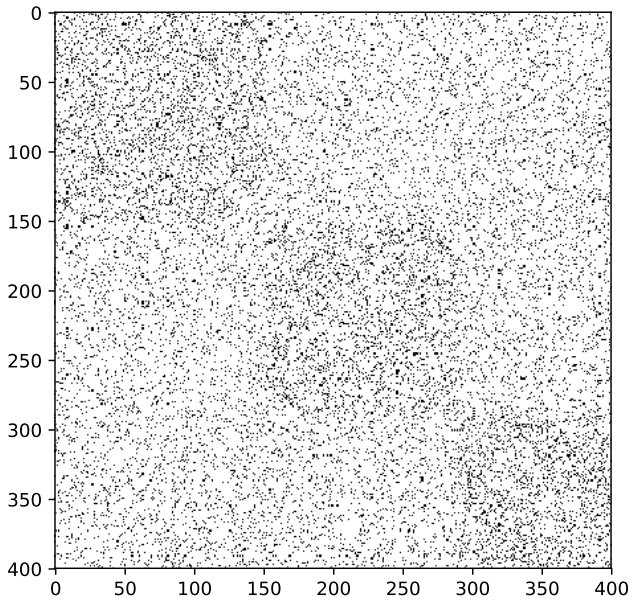

Figure 7: Adjacency matrix of random network.

```
import networkx as nx
n = 400
G = nx.erdos_renyi_graph(n, 0.1, seed=seed)
```

- Power-law network:

```
n = 400
G = nx.barabasi_albert_graph(n, 5, seed=seed)
```

- Small-world network:

```
n = 400
G = nx.newman_watts_strogatz_graph(400, 5, 0.5, seed=seed)
```

- Community network:

```
n1 = int(n/3)
n2 = int(n/3)
n3 = int(n/4)
n4 = n - n1 - n2 -n3
G = nx.random_partition_graph([n1, n2, n3, n4], .25, .01, seed=seed)
```

Initial values: We set the initial value $X(0)$ the same for all the experimental settings and thus different dynamics are only due to their different dynamic rules and underlying networks modelled by $\dot{X} = f(X, G, W, t)$ as shown in Fig. 2,3 and 4. Please see above animations to check out different network dynamics.

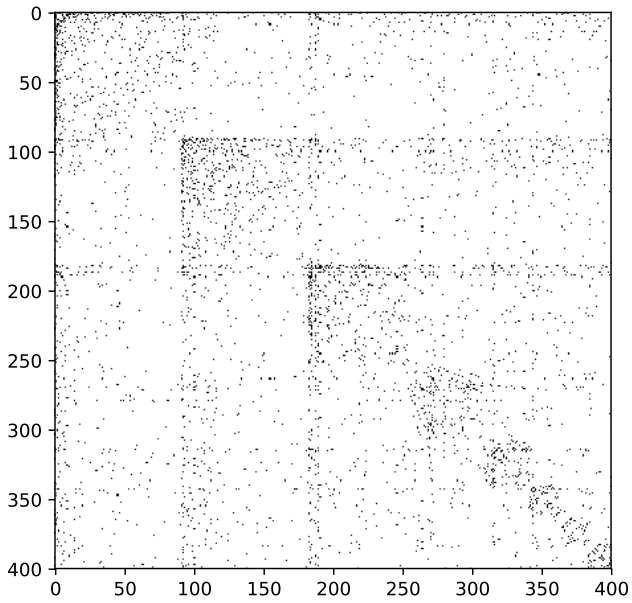

Figure 8: Adjacency matrix of power-law network.

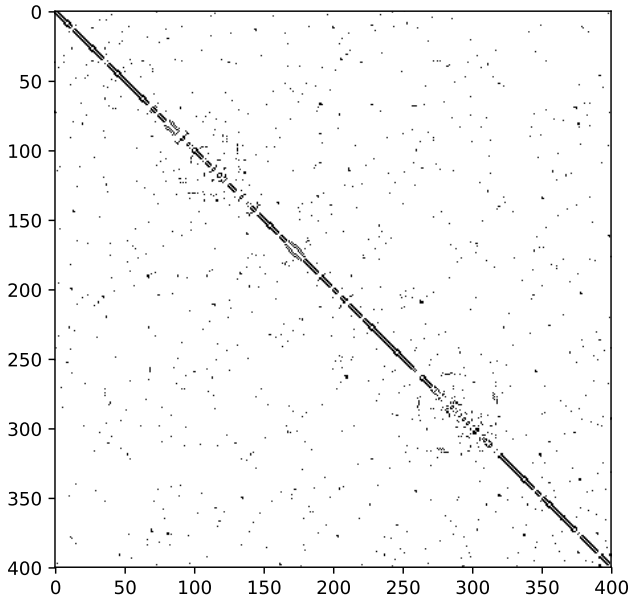

Figure 9: Adjacency matrix of small-world network.

```
n = 400
N = int(np.ceil(np.sqrt(n)))
x0 = torch.zeros(N, N)
x0[int(0.05*N):int(0.25*N), int(0.05*N):int(0.25*N)] = 25
# x0[1:5, 1:5] = 25  for N = 20 or n= 400 case
x0[int(0.45*N):int(0.75*N), int(0.45*N):int(0.75*N)] = 20
# x0[9:15, 9:15] = 20 for N = 20 or n= 400 case
x0[int(0.05*N):int(0.25*N), int(0.35*N):int(0.65*N)] = 17
# x0[1:5, 7:13] = 17 for N = 20 or n= 400 case
```

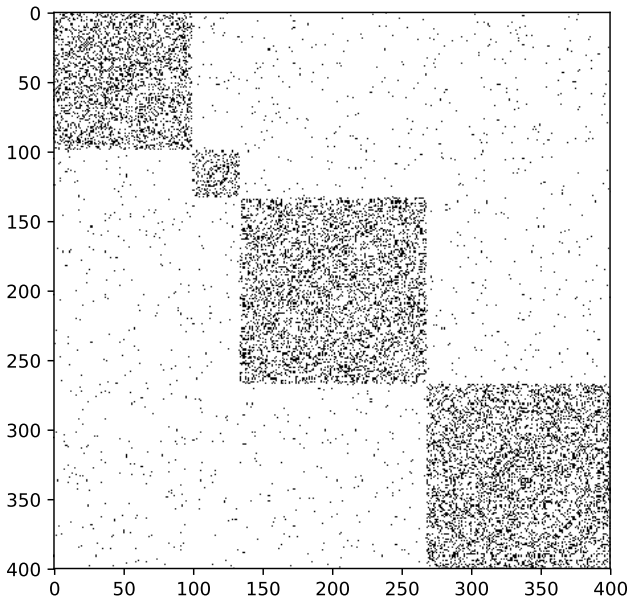

Figure 10: Adjacency matrix of community network.

Network Dynamics: We adopt following three real-world dynamics from different disciplines. Please see above animations to check out the visualization of different network dynamics. The differential equation systems are shown as follows:

- The heat diffusion dynamics governed by Newton's law of cooling [30],

$$\frac{d\overrightarrow{x_i(t)}}{dt} = -k_{i,j}\sum\nolimits_{j=1}^{n} A_{i,j}(\overrightarrow{x_i} - \overrightarrow{x_j}) \tag{10}$$

  states that the rate of heat change of node i is proportional to the difference in the temperatures between i and its neighbors with heat capacity matrix A. We use $k = 1$ here.
- The mutualistic interaction dynamics among species in ecology, governed by equation

$$\frac{d\overrightarrow{x_i(t)}}{dt} = b_i + \overrightarrow{x_i}(1 - \frac{\overrightarrow{x_i}}{k_i})(\frac{\overrightarrow{x_i}}{c_i} - 1) + \sum_{j=1}^{n} A_{i,j}\frac{\overrightarrow{x_i}\overrightarrow{x_j}}{d_i + e_i\overrightarrow{x_i} + h_j\overrightarrow{x_j}}. \tag{11}$$

  The mutualistic differential equation systems [17] capture the abundance $\vec{x_i}(t)$ of species i, consisting of incoming migration term b_i, logistic growth with population capacity k_i [51] and Allee effect [1] with cold-start threshold c_i, and mutualistic interaction term with interaction network A. We use $b = 0.1$, $k = 5.0$, $c = 1.0$, $d = 5.0$, $e = 0.9$, $h = 0.1$ here.
- The gene regulatory dynamics governed by Michaelis-Menten equation

$$\frac{d\overrightarrow{x_i(t)}}{dt} = -b_i\vec{x_i}^{\,f} + \sum\nolimits_{j=1}^{n} A_{i,j}\frac{\overrightarrow{x_j}^h}{\overrightarrow{x_j}^h + 1} \tag{12}$$

  where the first term models degradation when $f = 1$ or dimerization when $f = 2$, and the second term captures genetic activation tuned by the Hill coefficient h [17]. We adopt $b = 1.0$, $f = 1.0$, $h = 2.0$ here.

Terminal Time: We use $T = 5$ for mutualistic dynamics and gene regulatory dynamics over different networks, and $T = 5, 0.1, 0.75, 2, 0.2$ for heat dynamics on grid, random graph, power-law network, small-world network, and community network respectively due to their different time scale of network dynamics. Please see above animations to check out different network dynamics.

Visualizations of network dynamics: Please see above animations to check out the visualization of different network dynamics. We generate networks by aforementioned network models with 400 nodes. The nodes are re-ordered according to community detection method by Newman [32]. We visualize their adjacency matrices in Fig. 2,3 and 4. We layout these networks in a grid and thus nodes' states $X(t)$ are visualized as functions on the grid.

```
def generate_node_mapping(G, type=None):
    """
    :param G:
    :param type:
    :return:
    """
    if type == 'degree':
        s = sorted(G.degree, key=lambda x: x[1], reverse=True)
        new_map = {s[i][0]: i for i in range(len(s))}
    elif type == 'community':
        cs = list(community.greedy_modularity_communities(G))
        l = []
        for c in cs:
            l += list(c)
        new_map = {l[i]:i for i in range(len(l))}
    else:
        new_map = None

    return new_map


def networkx_reorder_nodes(G, type=None):
    """
    :param G:  networkX only adjacency matrix without attrs
    :param nodes_map:  nodes mapping dictionary
    :return:
    """
    nodes_map = generate_node_mapping(G, type)
    if nodes_map is None:
        return G
    C = nx.to_scipy_sparse_matrix(G, format='coo')
    new_row = np.array([nodes_map[x] for x in C.row], dtype=np.int32)
    new_col = np.array([nodes_map[x] for x in C.col], dtype=np.int32)
    new_C = sp.coo_matrix((C.data, (new_row, new_col)), shape=C.shape)
    new_G = nx.from_scipy_sparse_matrix(new_C)
    return new_G

G = networkx_reorder_nodes(G, args.layout)
A = torch.FloatTensor(nx.to_numpy_array(G))

def visualize_graph_matrix(G, title , dir=r'figure/network'):
    A = nx.to_numpy_array(G)
    fig = plt.figure()  # figsize=(12, 4), facecolor='white'
    fig.tight_layout()
    plt.imshow(A, cmap='Greys')  # ''YlGn')
    # plt.pcolormesh(A)
    plt.show()

def visualize_network_dynamics(N, x0, xt, figname, title ='Dynamics in Complex N
    """
    :param N:   N**2 is the number of nodes, N is the pixel of grid
    :param x0:  initial condition
    :param xt:  states at time t to plot
    :param figname:  figname , numbered
    :param title: title in figure
    :param dir: dir to save
    :param zmin: ax.set_zlim(zmin, zmax)
    :param zmax: ax.set_zlim(zmin, zmax)
    :return:
```

```
"""
if zmin is None:
    zmin = x0.min()
if zmax is None:
    zmax = x0.max()
fig = plt.figure()  # figsize=(12, 4), facecolor='white'
fig.tight_layout()
x0 = x0.detach()
xt = xt.detach()
ax = fig.gca(projection='3d')
ax.cla()
X = np.arange(0, N)
Y = np.arange(0, N)
X, Y = np.meshgrid(X, Y)
surf = ax.plot_surface(X, Y, xt.numpy().reshape((N, N)), cmap='rainbow',
                       linewidth=0, antialiased=False, vmin=zmin, vmax=zmax)
ax.set_zlim(zmin, zmax)
fig.savefig(dir+'/'+figname+".png", transparent=True)
fig.savefig(dir+'/'+figname + ".pdf", transparent=True)
# plt.draw()
plt.pause(0.001)
plt.close(fig)
```

C More results.

C.1 Results in absolute error.

We show corresponding ℓ_1 loss error with respect to normalized ℓ_1 loss error in Table 1.

Table 4: Our NDCN captures different network dynamics accurately. The mean fitting errors with standard deviation (in absolute error) in 20 runs measured by ℓ_1 loss.

		Grid	Random	Power Law	Small World	Community
Heat Diffusion	No-Embedding	1.095 ± 0.353	1.113 ± 0.021	1.083 ± 0.086	1.049 ± 0.196	1.256 ± 0.104
	No-Graph	1.509 ± 0.068	0.400 ± 0.052	0.603 ± 0.022	0.850 ± 0.018	1.037 ± 0.073
	No-Control	2.319 ± 0.034	1.331 ± 0.000	1.318 ± 0.019	1.524 ± 0.009	1.578 ± 0.016
	NDCN	$\mathbf{0.147 \pm 0.026}$	$\mathbf{0.274 \pm 0.009}$	$\mathbf{0.208 \pm 0.028}$	$\mathbf{0.129 \pm 0.021}$	$\mathbf{0.359 \pm 0.026}$
Mutualistic Interaction	No-Embedding	0.945 ± 0.114	2.558 ± 0.238	2.054 ± 0.727	0.887 ± 0.070	2.563 ± 0.460
	No-Graph	1.004 ± 0.185	1.173 ± 0.389	1.349 ± 0.191	0.803 ± 0.066	1.584 ± 0.108
	No-Control	2.058 ± 0.019	2.840 ± 0.033	3.320 ± 0.004	1.695 ± 0.015	3.488 ± 0.012
	NDCN	$\mathbf{0.287 \pm 0.046}$	$\mathbf{0.763 \pm 0.081}$	$\mathbf{0.528 \pm 0.041}$	$\mathbf{0.269 \pm 0.032}$	$\mathbf{0.767 \pm 0.042}$
Gene Regulation	No-Embedding	1.722 ± 0.533	3.818 ± 2.487	2.662 ± 0.721	1.262 ± 0.434	5.170 ± 1.945
	No-Graph	1.450 ± 1.666	3.905 ± 0.299	3.176 ± 0.083	0.713 ± 0.021	4.852 ± 0.046
	No-Control	3.056 ± 0.010	11.386 ± 0.138	3.586 ± 0.010	2.175 ± 0.005	9.891 ± 0.119
	NDCN	$\mathbf{0.312 \pm 0.031}$	$\mathbf{0.401 \pm 0.090}$	$\mathbf{0.221 \pm 0.016}$	$\mathbf{0.220 \pm 0.017}$	$\mathbf{0.516 \pm 0.065}$

C.2 Activation function

We find ReLU works better than $\tanh$ in the setting of learning network dynamics. We summarized the results in Table 5

C.3 Euler's method for NDCN

The results of our NDCN where the initial value problem in the forward process is solved by Euler's method are shown as follows:

Table 5: NDCN with $\tanh$ activation function. The mean fitting errors with standard deviation (in percentage $\%$) in 20 runs measured by normalized ℓ_1 loss.

		Grid	Random	Power Law	Small World	Community
Heat Diffusion	No-Embedding	43.7 ± 0.9	34.4 ± 0.0	34.0 ± 0.0	36.1 ± 0.1	41.9 ± 0.0
	No-Graph	38.9 ± 1.4	21.7 ± 0.3	17.3 ± 0.2	22.2 ± 0.1	31.8 ± 0.7
	No-Control	45.9 ± 0.2	27.3 ± 0.4	26.5 ± 0.1	31.5 ± 0.2	28.8 ± 0.5
	NDCN	$\mathbf{5.1 \pm 0.9}$	$\mathbf{20.9 \pm 0.3}$	$\mathbf{10.9 \pm 0.4}$	$\mathbf{6.9 \pm 1.2}$	$\mathbf{20.0 \pm 1.0}$
Mutualistic Interaction	No-Embedding	39.5 ± 0.0	22.5 ± 0.0	60.1 ± 0.2	40.1 ± 0.0	31.9 ± 0.1
	No-Graph	38.4 ± 0.1	12.6 ± 3.4	22.6 ± 1.7	37.4 ± 0.1	17.5 ± 3.8
	No-Control	39.1 ± 0.2	20.3 ± 0.1	45.0 ± 1.6	40.5 ± 0.2	28.8 ± 0.2
	NDCN	$\mathbf{10.6 \pm 0.7}$	$\mathbf{7.7 \pm 1.0}$	$\mathbf{10.2 \pm 0.4}$	$\mathbf{13.9 \pm 0.7}$	$\mathbf{9.7 \pm 0.5}$
Gene Regulation	No-Embedding	44.6 ± 0.7	40.5 ± 0.9	48.8 ± 0.0	37.5 ± 0.1	40.7 ± 0.7
	No-Graph	21.1 ± 0.1	15.9 ± 3.0	39.4 ± 0.1	15.5 ± 0.2	19.8 ± 0.7
	No-Control	48.5 ± 0.3	18.1 ± 1.0	18.0 ± 0.7	32.1 ± 1.3	23.9 ± 0.8
	NDCN	$\mathbf{5.3 \pm 0.5}$	$\mathbf{1.7 \pm 0.5}$	$\mathbf{3.4 \pm 0.2}$	$\mathbf{5.0 \pm 0.2}$	$\mathbf{1.7 \pm 0.3}$

Table 6: NDCN solved by Euler's method. The mean fitting errors with standard deviation (in percentage $\%$) in 20 runs measured by normalized ℓ_1 loss.

		Grid	Random	Power Law	Small World	Community
Heat Diffusion	No-Embedding	29.2 ± 12.6	29.4 ± 0.5	27.3 ± 0.2	28.6 ± 5.9	32.3 ± 2.3
	No-Graph	38.2 ± 0.6	10.4 ± 1.3	15.5 ± 0.1	21.4 ± 0.2	25.3 ± 0.9
	No-Control	58.8 ± 0.3	34.8 ± 0.0	34.7 ± 0.3	39.7 ± 0.2	41.4 ± 0.4
	NDCN	$\mathbf{5.0 \pm 0.4}$	$\mathbf{7.0 \pm 0.4}$	$\mathbf{5.1 \pm 0.2}$	$\mathbf{4.0 \pm 0.5}$	$\mathbf{9.5 \pm 0.9}$
Mutualistic Interaction	No-Embedding	35.1 ± 3.0	14.1 ± 2.1	35.0 ± 12.8	39.9 ± 3.3	21.9 ± 5.2
	No-Graph	35.2 ± 1.2	6.1 ± 0.3	20.1 ± 0.7	33.4 ± 1.1	12.3 ± 0.3
	No-Control	76.4 ± 0.3	22.1 ± 0.5	56.8 ± 0.1	72.5 ± 0.6	31.0 ± 0.5
	NDCN	$\mathbf{9.7 \pm 0.5}$	$\mathbf{4.6 \pm 0.3}$	$\mathbf{7.0 \pm 0.4}$	$\mathbf{10.6 \pm 0.4}$	$\mathbf{7.0 \pm 0.4}$
Gene Regulation	No-Embedding	34.1 ± 10.9	13.2 ± 11.3	33.3 ± 9.3	28.1 ± 9.3	17.3 ± 6.1
	No-Graph	21.0 ± 0.2	11.9 ± 0.1	39.3 ± 0.1	15.4 ± 0.2	19.1 ± 0.4
	No-Control	61.0 ± 0.1	31.7 ± 1.9	43.5 ± 0.2	47.6 ± 0.1	36.5 ± 0.5
	NDCN	$\mathbf{6.7 \pm 0.7}$	$\mathbf{1.3 \pm 0.2}$	$\mathbf{3.0 \pm 0.4}$	$\mathbf{4.8 \pm 0.4}$	$\mathbf{2.5 \pm 0.4}$

C.4 Kipf operator for NDCN

D Accuracy over terminal time and α

By capturing the continuous-time network dynamics, our NDCN gives better classification accuracy at terminal time $T \in \mathbb{R}^+$. Indeed, when the terminal time is too small or too large, the accuracy degenerates due to the fact that the features of nodes are in under-diffusion, or over-diffusion states. We plot the mean accuracy of 100 runs of our NDCN model over different terminal time T and α as shown in the following heatmap plots. we find for all the three datasets their accuracy curves follow rise and fall pattern around the best terminal time.

Table 7: NDCN solved by Euler method. The mean fitting errors with standard deviation (in percentage $\%$) in 20 runs measured by normalized ℓ_1 loss.

		Grid	Random	Power Law	Small World	Community
Heat Diffusion	No-Embedding	$\pm$	$\pm$	$\pm$	$\pm$	$\pm$
	No-Graph	$\pm$	$\pm$	$\pm$	$\pm$	$\pm$
	No-Control	$\pm$	$\pm$	$\pm$	$\pm$	$\pm$
	NDCN	$\pm$	$\pm$	$\pm$	$\pm$	$\pm$
Mutualistic Interaction	No-Embedding	$\pm$	$\pm$	$\pm$	$\pm$	$\pm$
	No-Graph	$\pm$	$\pm$	$\pm$	$\pm$	$\pm$
	No-Control	$\pm$	$\pm$	$\pm$	$\pm$	$\pm$
	NDCN	$\pm$	$\pm$	$\pm$	$\pm$	$\pm$
Gene Regulation	No-Embedding	$\pm$	$\pm$	$\pm$	$\pm$	$\pm$
	No-Graph	$\pm$	$\pm$	$\pm$	$\pm$	$\pm$
	No-Control	$\pm$	$\pm$	$\pm$	$\pm$	$\pm$
	NDCN	$\pm$	$\pm$	$\pm$	$\pm$	$\pm$

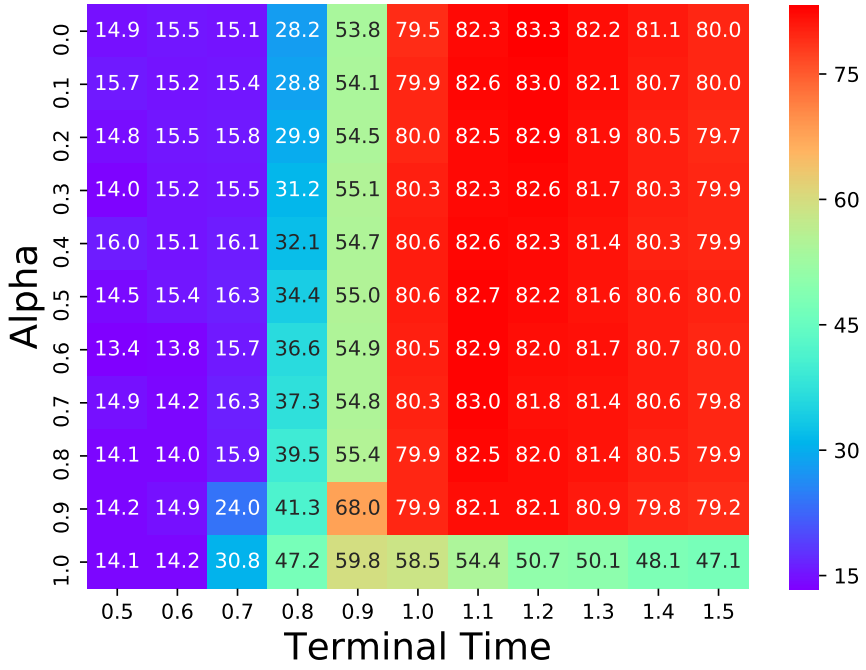

Figure 11: Mean classification accuracy of 100 runs of our NDCN model over terminal time and α for the Cora dataset in heatmap plot.

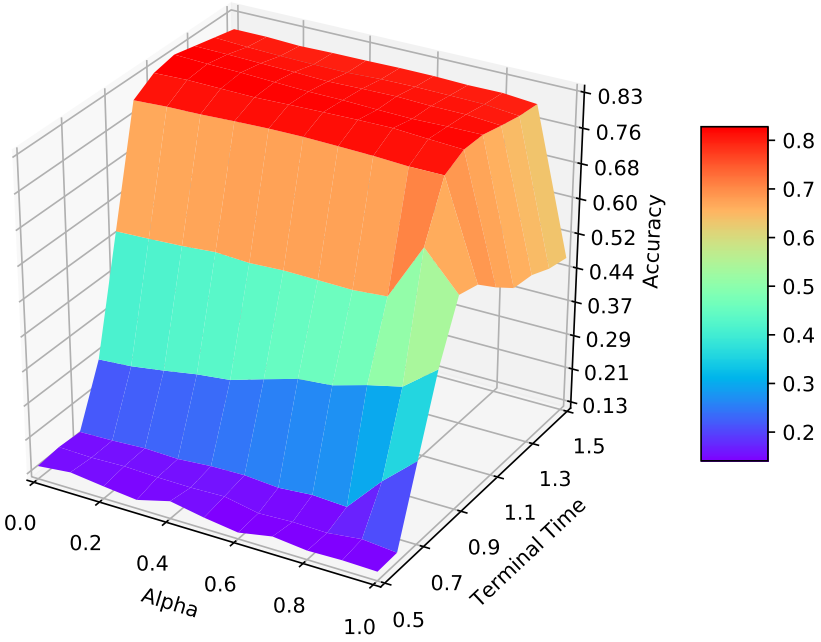

Figure 12: Mean classification accuracy of 100 runs of our NDCN model over terminal time and α for the Cora dataset in 3D surface plot.

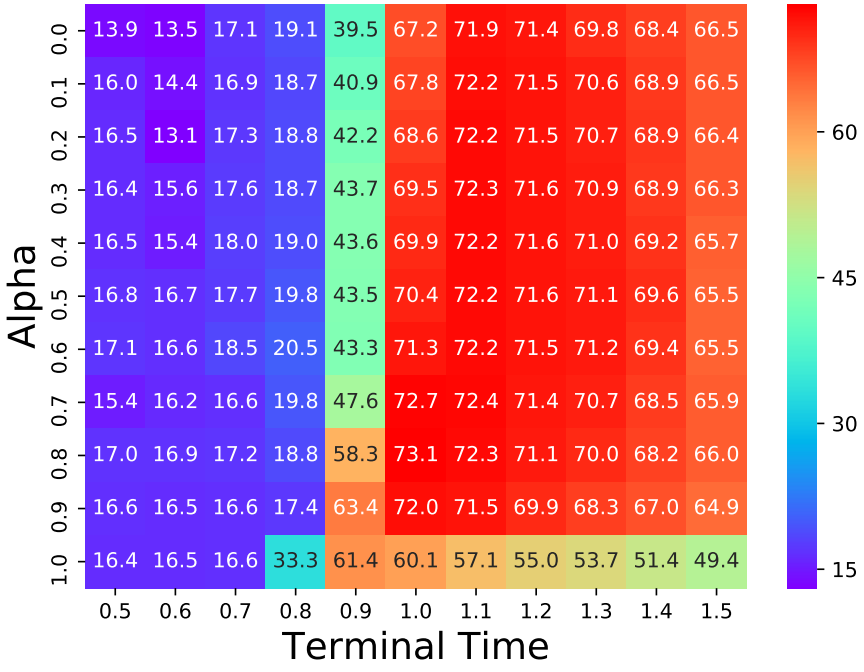

Figure 13: Mean classification accuracy of 100 runs of our NDCN model over terminal time and α for the Citeseer dataset.

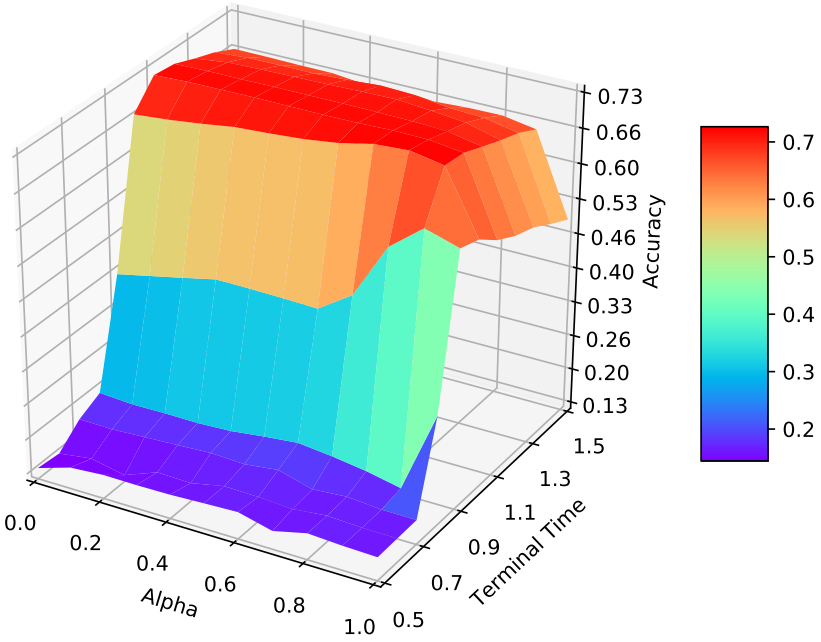

Figure 14: Mean classification accuracy of 100 runs of our NDCN model over terminal time and α for the Citeseer dataset in 3D surface plot.

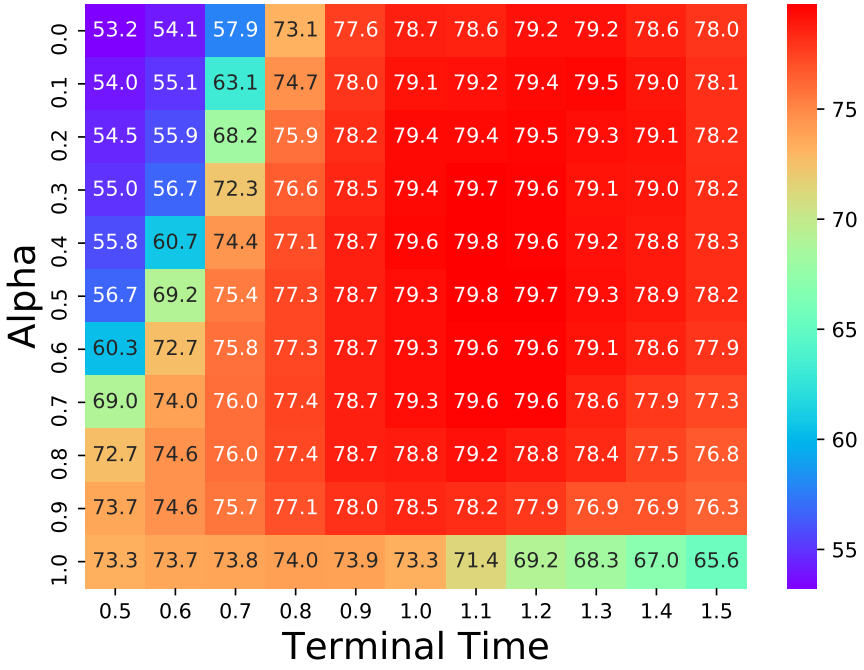

Figure 15: Mean classification accuracy of 100 runs of our NDCN model over terminal time and α for the Pubmed dataset.

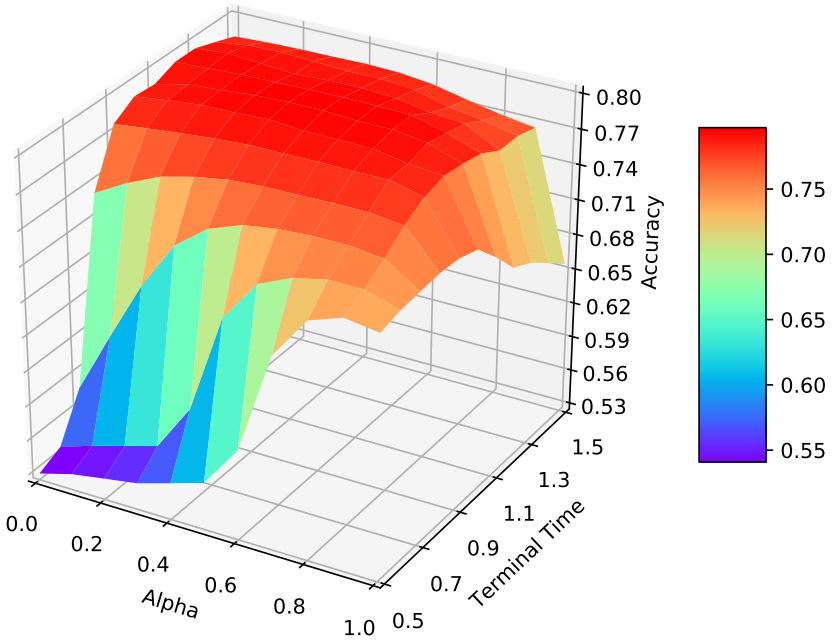

Figure 16: Mean classification accuracy of 100 runs of our NDCN model over terminal time and α for the Pubmed dataset in 3D surface plot.